Appl. Phys. A (2016) 122:840
DOI 10.1007/s00339-016-0320-4

Applied Physics A
Materials Science & Processing

Effect of Sb_2O_3 on the electrical properties of $Ba_{0.9}Ca_{0.1}Zr_{0.1}Ti_{0.9}O_3$ ceramics fabricated using nanocrystals seed

P. Parjansri[1] · U. Intatha[2] · R. Guo[3] · A. S. Bhalla[3] · S. Eitssayeam[4,5]

Received: 22 December 2015 / Accepted: 28 July 2016 / Published online: 22 August 2016

Abstract This work was to investigate the effects of antimony oxide (Sb_2O_3) on the electrical properties of $Ba_{0.9}Ca_{0.1}Zr_{0.1}Ti_{0.9}O_3$ (BCZT) ceramics and was prepared by adding 1 mol% of BCZT nanocrystals. The seed is nanocrystals of BCZT which was synthesized by the molten salt method. The ceramics powders were prepared by the mixed oxide method using $BaCO_3$, $CaCO_3$, ZrO_2, TiO_2 as starting materials, and the BCZT seed was added as nanocrystal for induce phase transition. They were doped with x mol% Sb_2O_3 ($x = 0.0$–0.5). Results indicated that all samples show pure perovskite phase. The Sb_2O_3 enhanced the electrical properties of the ceramic systems. Excellent values of a dielectric constant (ε_r) at room temperature (T_r) were 4086 with sample of $x = 0.5$, and at Curie temperature (T_c) was 15,485 for samples with $x = 0.1$. The highest remnant polarization (P_r), piezoelectric charge coefficient (d_{33}), piezoelectric voltage coefficient (g_{33}), electromechanical coefficient for planar mode (k_p) and thickness mode (k_t) values were 6.3 μC/cm^2, 346 pC/N, 15.6 × 10^{-3} Vm/N, 42 and 41 %, respectively, which were obtained for the sample of $x = 0.2$ mol% Sb.

1 Introduction

Lead-based piezoelectric ceramics have been widely used because of their excellent electrical properties such as high piezoelectric coefficient (d_{33}), high electromechanical properties (k_p and k_t), and which can be easily prepared forming perovskite phase structure. However, lead-based ceramics are not environmentally friendly because of the lead loss at high temperatures during the sintering process. Recently, lead-free piezoelectric ceramics have been extensively studied including $(K_{0.5}Na_{0.5})NbO_3$ (KNN), $(Na_{0.5}Bi_{0.5})TiO_3$, $(BaZr_xTi_{(1-x)}O_3$ (BZT) and $Ba_{(1-x)}Ca_xTiO_3$ (BCT) [1–4]. Liu and Ren [5] have reported that in $Ba_{(1-x)}Ca_xZr_{0.1}Ti_{0.9}O_3$ ceramics, the composition of x(Ca) = 0.15 gave the highest d_{33} value of 600 pC/N. However, it requires high calcination (1300–1350 °C) and sintering temperatures (1500–1550 °C) also using very long dwelling times for forming pure perovskite phase. Consequently, many researchers have focused on the study of the doping effects of various metal ions such as ZnO, CuO and La to reduce the calcination and sintering temperatures and also to improve the electrical properties of BCZT ceramics such as high dielectric constant (ε_r), remnant polarization (P_r), piezoelectric coefficient (d_{33}) and electromechanical factor (k_p and k_t) [6–8]. Moreover, a methodology of the synthesis piezoelectric ceramics with the forming pure perovskite phase at low calcinations temperature and also improves the electrical properties by modifying the textured structure of ceramics are applied by using the nanometric perovskite ceramics as a template added to the base ceramic component such as the seed-

✉ S. Eitssayeam
sukum99@yahoo.com

[1] Physics Division, Faculty of Science and Technology, Rajamangala University of Technology Krungthep, Bangkok 10120, Thailand

[2] School of Science, Mae Fah Luang University, Chiang Rai 57100, Thailand

[3] Department of Electrical and Computer Engineering, Faculty of Engineering, University of Texas at San Antonio, San Antonio, TX 78249, USA

[4] Department of Physics and Materials Science, Faculty of Science, Chiang Mai University, Chiang Mai 50200, Thailand

[5] Materials Science Research Center, Faculty of Science, Chiang Mai University, Chiang Mai 50200, Thailand

induced method and template grain growth [9–11]. Many researchers have carried out developing electrical properties of films by inserting a seed layer in a film preparation procedure for controlling the grain orientation and crystal orientation direction and also improving the ferroelectric and piezoelectric properties of films [12, 13]. It is well known that the seeding process in the case of ceramics helps to grow a single crystal template growth under controlled temperature conditions and the high electrical properties have been observed [11, 14, 15]. As reported by Li et al. [10], they added PT seed to the PZT ceramic and found that PZT ceramics can be formed in the pure perovskite phase at low calcination temperatures, and the samples showed high dielectric constant (ε_r) and low dielectric loss (tan δ). The addition of perovskite seed may play on important role in the powder preparation such as increasing the reactivity of precursor, the stabilization of perovskite phase, homogeneity of solid solution, calcinations and reducing the dwelling times; moreover, using the seed could improve the electrical properties of piezoelectric ceramics [10].

In our initial attempts, we have studied the seed-induced effects on $Ba_{0.9}Ca_{0.1}Zr_{0.1}Ti_{0.9}O_3$ (BCZT) ceramics by varying the seed content (0.0–4.0 mol%) and found that the pure perovskite phase can formed at low calcining temperatures with shorter dwelling times, and the densification, the microstructure as well as the electrical properties can be enhanced with the addition of BCZT perovskite seed. The maximum values of d_{33}, P_r, k_p and also low tan δ value were obtained at seed added BCZT sample (using the calcinations $\sim$1200 °C and sintering temperature $\sim$1450 °C). On the other hand, dielectric constant (ε_r) at room temperature of the seed added samples was lower than the non-seeded ceramics. From the previous results, the doping of metal oxide to enhance the dielectric constant and also other electrical properties will be investigated. The metal oxide is proposed as Sb_2O_3-doped piezoelectric ceramics have been reported [16–20]. The Sb_2O_3 was used as doping agent in many piezoelectric systems to enhance the dielectric and other electrical properties [16–20]. Chan et al. [16] reported that $(Na_{0.5}K_{0.5})Nb_{(1-x)}Sb_xO_3$ ceramics exhibited high values of $d_{33} \sim 123$ pC/N, $k_p \sim 42$ %, $\varepsilon_r \sim 446$ and tan $\delta \sim 0.0023$ for a sample with Sb(x) = 0.03. Lin et al. [17] showed that a sample of Sb (x) = 0.06 in a system of $(K_{0.5}Na_{0.5})_{0.94}$-$Li_{0.06}(Nb_{1-x}Sb_x)O_3$ ceramic resulted $d_{33} \sim 212$ pC/N, $k_p \sim 46$ % and $k_t \sim 47$ %. Rani et al. [18] studied $[Na_{0.5}K_{0.5}]_{1-x}Li_x[Sb_xNb_{1-x}]O_3$ ceramics and found that the sample with Sb (x) = 0.05 had a maximum remnant polarization (P_r) $\sim$ 0.66 μC/cm^2 and $d_{33} \sim 273$ pC/N. Petrovic et al. [19] studied Sb-doped $BaTiO_3$ ceramic. It was found that grain size decreased with increasing Sb doping with the highest ε_r value for the sample with 0.3 mol% Sb. Also, Sb affects the ferroelectric properties of the ceramics, changing the normal ferroelectric to relaxor ferroelectric when high Sb content in $[Pb_{0.92}(La_{1-x}Sb_x)_{0.089}Zr_{0.65}Ti_{0.35})_{0.98}]O_3$ ceramic was used [20]. The above literature stated that proper Sb doping can enhance the electrical properties of many perovskite piezoelectric ceramics such as remnant polarization (P_r), piezoelectric coefficient (d_{33}) and electromechanical coupling coefficient (k), also the grain size is greatly decreased with higher Sb content while showing high dielectric constants. Thus, Sb-doped ceramics may be of interest. In this work, we have focused on the investigation of the effect of Sb oxide on the electrical properties of $Ba_{0.9}Ca_{0.1}Zr_{0.1}Ti_{0.9}O_3$ ceramic adding 1.0 mol% of BCZT seed and prepared by still using the calcinations temperature at 1200 °C, dwelling time for 2 h and using different of the sintering temperature (1440 °C for 2 h), because the sample melts at the sintering temperature of 1450 °C which use in the previous work (prepared by seed-induced method).

2 Experiment

2.1 Synthesis of Sb_2O_3-doped BCZT ceramics

The BCZT seed-induced ceramics were prepared by using their own nanocrystals to help to form a pure perovskite phase at low calcinations temperatures. This technique is similar to the conventional method, but the difference is using their own nanocrystals to help as nuclei or seed, which will refer as the seed-induced method. In this work, we studied the effect of Sb_2O_3 on the properties of $Ba_{0.9}Ca_{0.1}Zr_{0.1}Ti_{0.9}O_3$ (BCZT) ceramics induced by using BCZT seed. The BCZT seed as a raw material was synthesized from $Ba_{0.9}Ca_{0.1}Zr_{0.1}Ti_{0.9}O_3$ by the molten salt route. The starting powders of seed were calculated and weighed, and after that were mixed with KCl–NaCl salt (1:1) then the mixed powder was heated at 1000 °C for 2 h. After that, they were washed with hot deionized water several times until no trace of anion and dried in an oven at 120 °C. Next state, the raw materials of $BaCO_3$ (Sigma-Aldrich, >99 %), $CaCO_3$ (Sigma-Aldrich, 98.5–100.5 %), ZrO_2 (Sigma-Aldrich, >99 %), TiO_2 (Sigma-Aldrich, 99–105.5 %), Sb_2O_3 (Fluka, ≥99 %) and BCZT seed were mixed. They were ball-milled for 24 h in ethanol with zirconia grinding media. This system, the BCZT nanocrystals were added at 1 mol% for all conditions of doping of Sb_2O_3. The dopant Sb_2O_3 was in the ratio of Sb (x) = 0.0, 0.1, 0.2, 0.3 and 0.5 (x mol%). The powders were dried and calcined in crucibles at 1200 °C for 2 h. Then the BCZT seed-induced powder doped with Sb_2O_3 powders was

mixed with an organic binder and pressed into pellets. The pellets were sintered at 1440 °C for 4 h with a heating/cooling rate of 5 °C/min.

2.2 Characterization

Phase formation and microstructure of the samples were investigated by X-ray diffraction (XRD) (X'Pert PANalytical) and scanning electron microscopy (SEM). For electrical property characterization, the sintered ceramics were ground to obtain parallel faces and the faces were coated with silver as electrodes. The dielectric constants and dielectric loss of the sintered ceramics were measured as a function of frequency and temperature with an automated dielectric measurement system (4284A Precision LCR meter, Hewlett Packard). The samples were characterized for ferroelectric properties by hysteresis loop using a precision workstation (Radiant technology Inc.). The range in electrical field of −15 to 15 kV/cm and at room temperature was used. After that, the specimens were poled by applying a DC field of 3 kV/mm for 30 min in a silicone oil bath at 28 °C by using a HV supply amplifier/controller (Trek model 610D). Finally, the poled samples were characterized for piezoelectric properties using a ZJ-4B piezo d_{33} m (IACAS) and the electromechanical coupling coefficients k_p, k_t and Q_m of the poled samples were investigated by a resonance and anti-resonance method by using a 4194A impedance analyzer.

3 Results and discussion

3.1 Phase structure, microstructure and density analysis

The phase formation of bulk ceramic samples was analyzed by X-ray diffractometer (XRD) as shown in Fig. 1. It was found that all samples were pure perovskite phase without a secondary phase and showed peaks corresponding to the perovskite peaks of (100), (110), (002)/(200) and (210) (JC-file standard). The pure perovskite phase in the ceramic systems indicated that the Sb ion had successfully diffused into the BCZT lattice [16, 18] and also the adding BCZT seed help to increase the reactivity of precursor, the stabilization of perovskite phase, homogeneity of solid solution [10]. The enlarged XRD patterns for $2\theta = 44°–46°$ showed that the peak gradually split for (002)/(200) reflections with increasing Sb. This result indicates that the ceramics exhibited the existence of both rhombohedral and tetragonal phases [5]. The diffraction peaks slightly shifted with increasing Sb doping may be due to the different ion radius of Sb^{3+}, Ba^{2+} and Ti^{4+} [16, 18]. The Sb ion may be modifying texture of BCZT ceramic, leading to the change in density and grain size values as data are listed in Table 1 and Fig. 2. The density and grain size values of all samples displayed in Fig. 2. It was found that Sb content at 0.1 mol% in both the density and grain size increased; however, the Sb content increased from $x = 0.2$ to $x = 0.5$; the density values are not significantly changed, while the grain size clearly decreased. The density values are in the range of 5.61–5.73 g/cm^3, and the grain size values are in the range of and 2.55–14.35 μm (Table 1). The highest density and grain size values were found for the samples with $x = 0.1$ and $x = 0.2$, respectively. The lowest density was for sample with $x = 0.2$, while grain size was large. Small voids possibly occur in grain boundaries for this sample [9]. From grain size results, decreases in grain size could be a result of more Sb content which resulted in a reduced vacancies diffusion coefficient (the lattice diffusion of vacancies from pore to grain boundaries leads to the grain growth during sintering) and Sb particles accumulated near grain boundaries. Thus, leading the grain growth to be suppressed [21, 22]. The decreasing grain size with increasing Sb doping in this study is similar to work reported by Rani et al. [18] and Ma et al. [23].

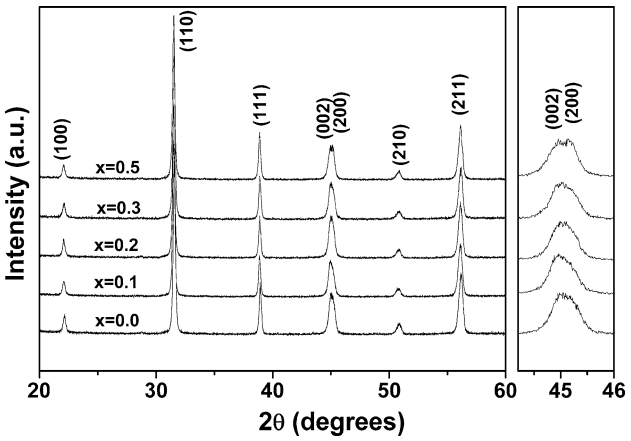

Fig. 1 XRD patterns and expanded XRD patterns for $2\theta = 44°–46°$ for doped BCZT ceramic samples (x = mol% Sb_2O_3)

3.2 Dielectric properties

Figure 3 shows the plots of the dielectric properties (at 1 kHz) as a function of Sb content which were measured at room temperature (T_r) and Curie temperature (T_c) (as shown in Fig. 3a, b, respectively). Results showed that at T_r, the dielectric constant (ε_r) and dielectric loss (tan δ) tended to increase with increasing Sb content with values in the range of 2149–4086 and 0.008–0.036, respectively. The increasing dielectric properties (ε_r and tan δ values) may be due to the decreasing grain size [18, 24]. These results might also arise from the Sb ion as it has a different valence and substitution size when it enters at the A-site or

Table 1 Density, grain size and dielectric properties of Sb(x)-doped BCZT samples

Samples (x)	Density (g/cm^3)	Grain size (μm)	At T_r		At T_c		T_c (°C)	γ	δ
			ε_r	tan δ (%)	ε_r	tan δ (%)			
0.0	5.70	7.93	2149	0.85	14,337	1.12	89	1.69	11.34
0.1	5.73	13.86	2220	1.28	15,485	1.11	92	1.55	8.12
0.2	5.61	14.35	2377	1.36	14,088	1.21	80	1.77	13.17
0.3	5.64	4.63	3291	2.69	12,820	1.65	72	1.91	20.16
0.5	5.65	2.55	4086	3.82	10,227	2.93	64	1.73	19.93

T_r is room temperature

T_c is Curie temperature (maximum dielectric temperature)

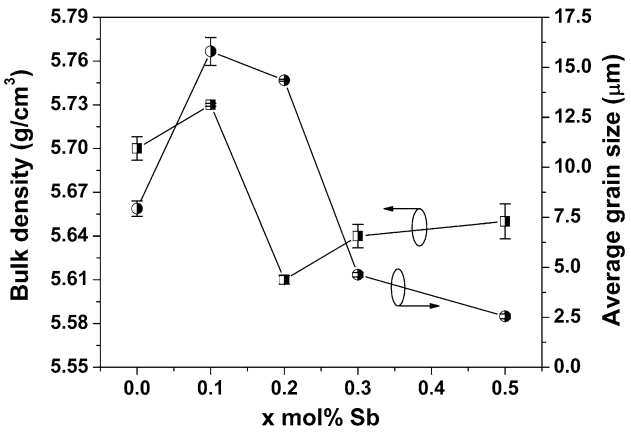

Fig. 2 Bulk density and average grain size values as a function of mol% Sb in BCZT

B-site of the BCZT structure; creating oxygen or ion vacancies and inner stress in the lattice structure. It is well known that the Sb^{3+} ion at the A-site creates a donor effect, and at the B-site creates an acceptor effect causing ion (V''_{Ba}) and oxygen ($V^{\circ\circ}_{Ti}$) vacancies and can also be described by [22–27]:

$$Sb_2O_3 \rightarrow 2Sb^{3+}_{Ba^{2+}} + 3O_0 + V''_{Ba} \quad (1)$$

$$Sb_2O_3 \rightarrow 2Sb^{3+}_{Ti^{4+}} + 3O_0 + V^{\circ\circ}_{Ti} \quad (2)$$

As mentioned above, the higher dielectric constant and dielectric loss at room temperature may be the result of the ions and oxygen vacancies when Sb was doped in BCZT ceramics. At T_c, while Sb content increased; the ε_r increases from $x = 0.0$ to $x = 0.1$ and then it decreased rapidly with increasing of Sb content. The highest dielectric constant of 15,485 was obtained for the sample with $x = 0.1$ mol%. For tan δ behavior, the values tended to increase with increasing Sb content; however, these systems exhibited values of tan δ lower than 0.03 for all samples. It can be noted that Sb-doped BCZT ceramics improved the dielectric constant for suitable content of Sb. On the other hand, the higher Sb content might create more oxygen vacancies in the BCZT structure leading to the drop of dielectric constant at high temperature.

The dielectric properties of the BCZT ceramic systems were measured as a function of temperature in the range of −100 to 150 °C and are shown in Fig. 4. From the figure, the ceramics exhibited two phase transitions corresponding to the rhombohedral–tetragonal (T_{R-T}) at ~45–50 °C

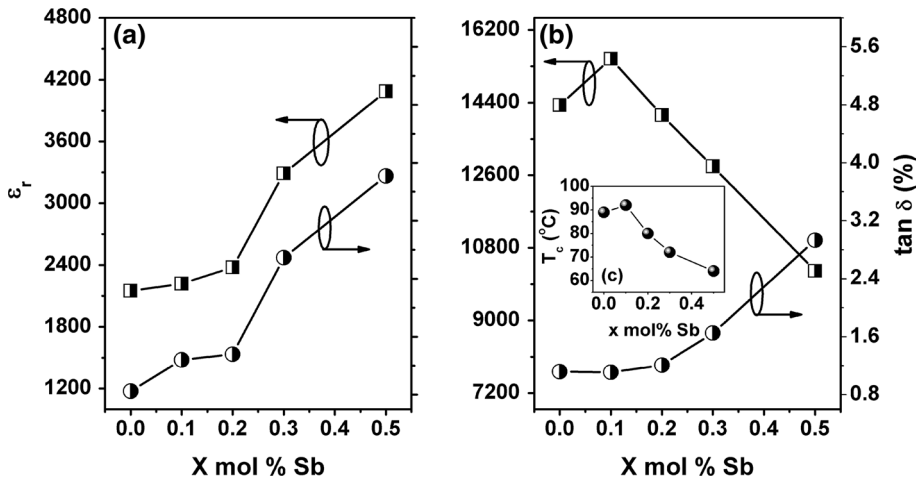

Fig. 3 Dielectric constant (ε_r), dielectric loss (tan δ): **a** at room temperature, **b** at maximum temperatures and Curie temperature (T_c) *inset* **c** for various BCZT:Sb ceramics

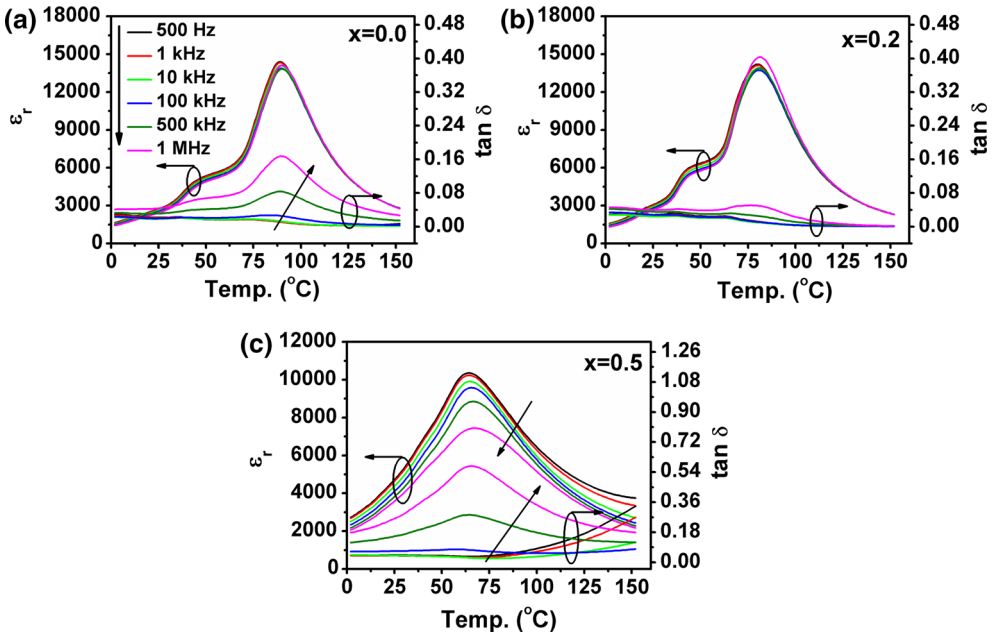

Fig. 4 Dielectric constant (ε_r) and dielectric loss (tan δ) as a function of temperature for BCZT:Sb ceramics: **a** No–Sb, **b** 0.2 mol% Sb and **c** 0.5 mol%

phase and tetragonal–cubic (T_c) phase transitions at 89 °C for the sample of $x = 0.0$ and at 64 °C with 0.2 mol% Sb. With the increase in Sb content to 0.5 mol%, the transition from rhombohedral to tetragonal phase was not observed. The tetragonal–cubic (T_c) phase transitions temperature was reduced to a lower temperature from 92 to 64 °C with increasing Sb content as shown in inset (Fig. 3b) and Table 1. The T_c decrease may be due to the substitution of Sb^{3+} ions (Sb^{3+} ions occupy the A-site or B-site in lattice randomly) leading to the deformation of the ABO_3 lattice and the appearance of ion vacancies when the Sb content was increased [5, 27, 28]. These results correspond with the decrease in density and grain size values; thus, it should be noted that the increasing Sb content had an effect on the phase formation from tetragonal to cubic phase shifting to lower temperatures. Moreover, the maximum dielectric constant for $x = 0.0$ to $x = 1.0$ mol% increased and then reduced with increasing Sb content for samples of 0.2–0.5 mol% Sb and subsequently the dielectric peak became broader with temperature and clearly dependent on the frequency for sample with $x = 0.5$. Such behavior suggests that the diffuseness of the phase transition relates to the relaxor-like behavior for these compositions [29]. To further understand the broadening and dispersion of the maximum dielectric peak with frequency, a modified Curie–Weiss law was used for the analysis of these results [29]:

$$\frac{\varepsilon_m}{\varepsilon(f,T)} = 1 + \frac{(T - T_m(f))^\gamma}{2\delta^2} \quad (3)$$

where ε_m is the maximum value of the dielectric constant at $T = T_m(f)$. The value of γ in the expression is the degree of dielectric relaxation, while δ is used to measure the degree of diffuseness of the phase transition. The slope of the fitting curves using Eq. 3 determines the γ and the δ values. When $\gamma = 1$, it is a normal Curie–Weiss behavior (pure ferroelectric behavior), and when $\gamma = 2$ it is identical to the quadratic relationship (a complete diffuse phase transition). The values of γ and δ for these ceramic are show in Table 1. It was found that γ and δ values changed with Sb content, from 1.55 to 1.91 and 8.12–20.16, respectively. The increase in γ and δ values with Sb content suggests that high degrees of relaxor ferroelectric-like behavior and phase transition diffuseness occurred in BCZT ceramics. The relaxor likes the behavior results from the unbalance of charges and lattice disorder after BCZT was doped with the higher Sb content leading to high inner stress in the structure and weak long-range interactions [30, 31]. For the tan δ result, similar behavior as that of the dielectric constant is seen. Sb doping reduced the dispersion with the frequency of tan δ which was observed for samples with 0.1 and 0.2 mol% of Sb. As a result, it can be noted that the Sb doping changed and also improved the dielectric properties of BCZT ceramics at maximum temperature.

3.3 Ferroelectric properties

Figure 5 illustrates the ferroelectric properties of BCZT ceramics doped with Sb; P–E hysteresis loop (Fig. 5a) and remnant polarization (P_r) and coercive field (E_c) (Fig. 5b).

It was found that all samples have a slim ferroelectric behavior. The P_r values increased with increasing Sb doping from $x = 0.0$ to $x = 0.2$ and then decreased with increasing Sb content. The decreasing P_r values for samples of $x = 0.3$ and $x = 0.5$ may be due to the increase in vacancies and impurities with higher Sb content and also related to the greatly decreased grain size value resulting in the decrease in grain boundary mobility [23, 32]. The higher P_r value for samples of $x = 0.1$ and $x = 0.2$ was because of reversible movement of the domain wall and the increase in the domain reorientation during the applied electric field cycle [33, 34]. The highest P_r values of 6.3 μC/cm^2 were obtained for the sample with $x = 0.2$. For the E_c parameter, it was found that Sb doping had little effect on the E_c value; however, these ceramics show E_c values lower than 2.0 kV/cm.

3.4 Piezoelectric and electromechanical properties

The piezoelectric and electromechanical properties of BCZT ceramics doped with Sb are shown in Figs. 6 and 7, respectively. Figure 6 shows the piezoelectric charge coefficient (d_{33}) and piezoelectric voltage coefficient (g_{33}) as a function of Sb content. The d_{33} values increased with increasing Sb content from x = 0.0 to $x = 0.2$ mol% and then decreased with increasing in Sb content. The highest d_{33} value of 346 pC/N was obtained for $x = 0.2$ sample. The g_{33} value also showed the same trend as the behavior of d_{33} values for all samples. The g_{33} values were determined by using expression (4) [25]:

$$g_{33} = \frac{d_{33}}{\varepsilon_0 \varepsilon_r} \tag{4}$$

where ε_o is permittivity of a free space, and ε_r is relative permittivity. The values of ε_r were measured at room temperature. The g_{33} values were calculated at room

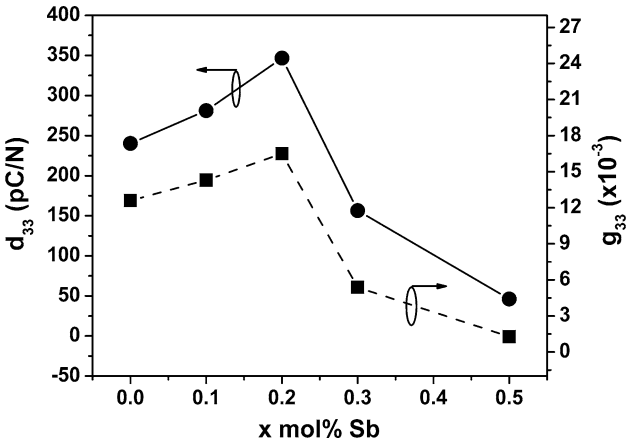

Fig. 6 Piezoelectric charge coefficient (d_{33}) and piezoelectric voltage coefficient (g_{33}) of BCZT:Sb ceramics

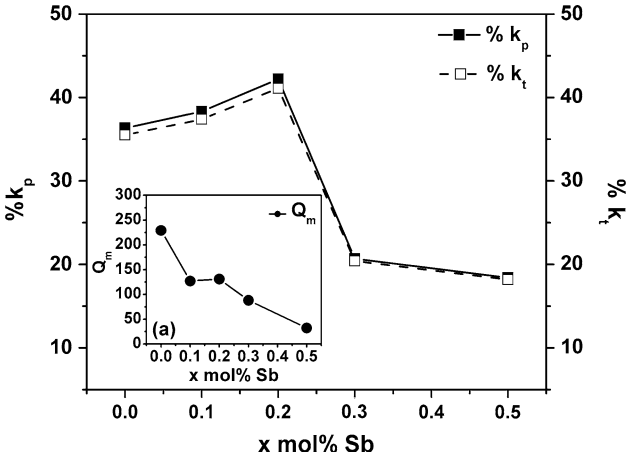

Fig. 7 Electromechanical coupling coefficient: planar mode (k_p) and thickness mode (k_t). *Inset* **a** mechanical factor (Q_m) for BCZT:Sb ceramics

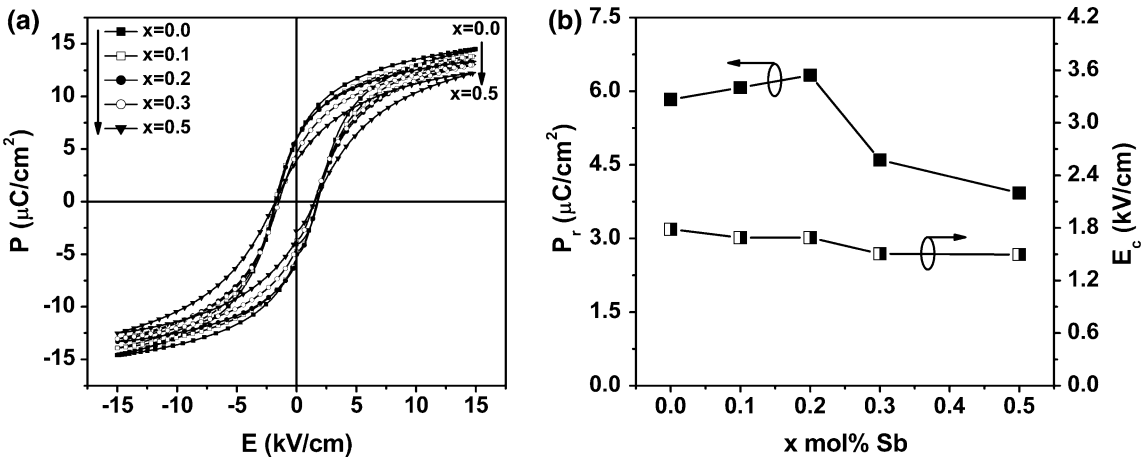

Fig. 5 Ferroelectric properties of BCZT:Sb ceramics: **a** P–E hysteresis loops, and **b** remnant polarization (P_r) and coercive field (E_c)

temperature and were in the range of 5.37×10^{-3}–16.5×10^{-3} Vm/N. The highest value was obtained for the sample with $x = 0.2$ mol%. From the results of d_{33} and g_{33} values, it can be suggested that Sb doping may also be related to the domain movement mechanism as the domain wall motion depends on the grain size (grain size increase leads to the increase in domain size and decrease in the grain boundaries number) [35]. Consequently, the highest d_{33} and g_{33} values were obtained for the large grain size sample ($x = 0.1$ and $x = 0.2$ mol%) as shown in Fig. 2. Hence, the increase in domain wall movement with increasing grain size leads to the easier poling process [35–37]. Also, the higher d_{33} for small Sb content may be attributed to the coexistence of rhombohedral and tetragonal phases near room temperature [36, 38, 39]. On the other hand, the decreases in d_{33} and g_{33} for samples with $x = 0.3$ to $x = 0.5$ may be due to the small grain size and low remnant polarization (P_r) which results in more difficult domain motion, grain orientation and polarization switching in the poling process [32, 35–37]. The electromechanical properties, including the planar mode coupling coefficient (k_p) and thickness mode coupling coefficient (k_t), are shown in Fig. 7. The k_p and k_t values were analyzed from the impedance spectra and calculated through equation as following the IEEE standards [40]. Figure 7 shows that k_p and k_t follow similar behavior to the piezoelectric properties for all conditions. The k_p and k_t values tended to increase from 36 to 42 % and 35.5 to 41.1 %, respectively, for samples with $x = 0.0$ to $x = 0.02$ mol% Sb, and then these values decrease with increasing Sb content. The electromechanical properties (k coefficient) could be determined by the polarization process, while the electric field was applied during the poling process.

The relationship of impedance spectra (a) and phase angle (b) around the resonance and anti-resonance mode with frequency is shown in Fig. 8. A phase angle close to 90° and in a large frequency range for anti-resonance as well as resonance frequencies was found for samples with $x = 0.0$ to $x = 0.2$ and is related to the high k_p and k_t values for these samples (seen in Fig. 8c). According to theory, it is well known that the phase angle approaches 90° for the ceramics which were fully poled (ideal poling state) [41]. Thus, Sb doping in BCZT improves the domain switching in the poling process. The decrease in k coefficient values may be due to the higher amount of Sb content which created more oxygen vacancies and affected the domain wall mechanically [37, 42, 43]. The Q_m values [inset (a) in Fig. 7] were calculated by using the expression (5) [40],

$$Q_m = \frac{f_a^2}{2\pi Z_m C f_r (f_a^2 - f_r^2)} \quad (5)$$

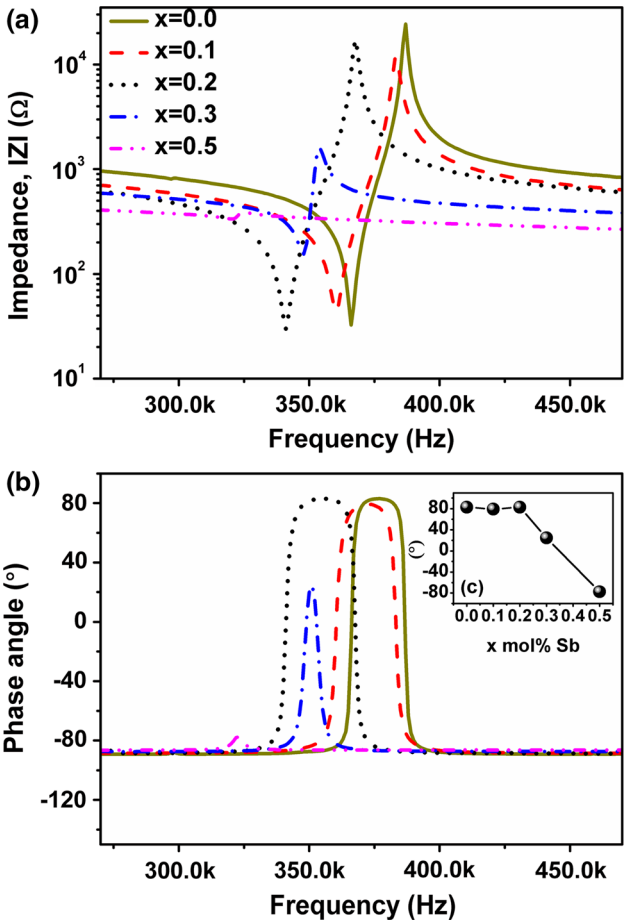

Fig. 8 Impedance (Z), **a** and phase angle (°), **b** as a function of frequency for BCZT: Sb (x mol%) ceramics. *Inset* **c** phase angle values with x mol% Sb

where Z_m is the impedance at resonance frequency (Ω), and C is the capacitance at room temperature and 1 kHz. The Q_m parameter indicates the sharpness of electromechanical resonance spectra. Also, the Q_m value can be defined in terms of the mechanical loss which is the proportion of Q_m^{-1} [44]. Thus, when increasing the Sb content from $x = 0.0$ to $x = 0.5$ the Q_m value tended to decrease. The Q_m values were in the range of 32.2–229. The decreasing Q_m values resulted from the increasing mechanical loss which may be due to the high dielectric loss for samples doped with higher Sb content.

4 Conclusions

The effect of antimony (Sb_2O_3) doping on the electrical properties of BCZT ceramics produced by the adding 1.0 mol% of BCZT seed was investigated. It was found that ceramics showed a pure perovskite phase as well as the existence of rhombohedral and tetragonal phases. The

density values are in the range of 5.61–5.73 g/cm^3, and the grain size values are in the range of and 2.55–14.35 μm. The dielectric constant (ε_r) measured at room temperature was in the range of 2149–4086 for the samples of $x = 0.0$ to $x = 0.5$. The Sb-doped samples show higher ε_r value which is comparable properties with the un-doped sample ($x = 0.0$). The tan δ values were lower than 0.04 for all samples. The highest values of $P_r = 6.3$ μC/cm^2, $d_{33} = 346$ pC/N, $g_{33} = 16.5 \times 10^{-3}$ Vm/N, $k_p = 42$ % and $k_t = 41$ %, respectively, were obtained for the sample with 0.2 mol% Sb. Results suggested that the sample of $x = 0.2$ mol% should have better piezoelectric material. Also, the higher Sb content samples showed high degrees of relaxor ferroelectric behavior. Results concluded that Sb doping with using the nanocrystal perovskite BCZT as a seed can enhance the piezoelectric and electromechanical properties of these ceramics, especially the dielectric constant can compared with the BCZT ceramic only adding the BCZT seed (the sample without Sb_2O_3). Also, this ceramic system still using low calcination temperature and short dwelling time for forming pure perovskite phased with using seed-induced method.

Acknowledgments The authors would like to thank the Thailand Research Fund (TRF) grant no. TRG5780013 for financial support, including the support given through the Royal Golden Jubilee Ph.D. Program, Office of the Higher Education Commission, Thailand, Multi-Functional Electronic Material and Device Research Lab (UTSA) through NSF/INAMM, Science and Technology Research Institute, Chiang Mai University and the Faculty of Science and Graduate School, Chiang Mai University, Mae Fah Luang University.

References

1. L. Egerton, D.M. Dillon, J. Am. Ceram. Soc. **42**, 438 (1959)
2. G.O. Jones, P.A. Thomas, Acta Crystallogr. **B56**, 426 (2000)
3. D. Hennings, A. Schnell, G. Simon, J. Am. Ceram. Soc. **65**, 539 (1982)
4. X. Wang, H. Yamada, C.N. Xu, Appl. Phys. Lett. **86**, 022905 (2005)
5. W. Liu, X. Ren, Phys. Rev. Lett. **103**, 257602 (2009)
6. J. Wu, D. Xiao, W. Wu, Q. Chen, J. Zhu, Z. Yang, J. Wang, Scr. Mater. **65**, 771 (2011)
7. Q. Lin, M. Jiang, D. Lin, Q. Zheng, X. Wu, X. Fan, J. Mater. Sci. Mater. Electron. **24**, 734 (2013)
8. T. Chen, T. Zhang, G. Wang, J. Zhou, J. Zhang, Y. Liu, J. Mater. Sci. **47**, 4612 (2012)
9. P. Parjansri, K. Pengpat, G. Rujijanagul, T. Tunkasiri, U. Intatha, S. Eitssayeam, Ferroelectrics **458**, 91 (2014)
10. Z. Li, A. Wu, P.M. Vilarinho, Chem. Mater. **16**, 717 (2004)
11. S.K. Ye, J.Y.H. Fuh, L. Lu, Appl. Phys. Lett. **100**, 252906 (2012)
12. Y.-J. Son, Y.-J. Kim, B.-H. Lee, S.-Y. Hwang, N.-K. Park, H.-Y. Chang, S.-K. Hong, S.J. Hong, J. Korean Phys. Soc. **51**, 701 (2007)
13. L.M. Sanchez, D.M. Potrepka, G.R. Fox, I. Takeuchi, K. Wang, L.A. Bendersky, R.G. Polcawich, J. Mater. Res. **28**, 1920 (2013)
14. J.A. Horn, S.C. Zhang, U. Selvaraj, G.L. Messing, S. T-McKinstry, J. Am. Ceram. Soc. **82**, 921 (1999)
15. C. Duran, S. T-McKinstry, G.L. Messing, J. Am. Ceram. Soc. **83**, 2203 (2000)
16. I.-H. Chan, C.-T. Sun, M.-P. Houng, S.-Y. Chu, Ceram. Int. **37**, 2061 (2011)
17. D. Lin, K.W. Kwok, K.H. Lam, H.L.W. Chan, J. Phys. D Appl. Phys. **40**, 3500 (2007)
18. R. Rani, S. Sharma, R. Rai, A.L. Kholkin, Mater. Res. Bull. **47**, 381 (2012)
19. M.M. Vijatović Petrović, J.D. Bobić, J. Banys, B.D. Stojanović, Mater. Res. Bull. **48**, 3766 (2013)
20. S. Dutta, R.N.P. Choudhary, P.K. Sinha, Mater. Sci. Eng. B **113**, 215 (2004)
21. R.B. Atkin, R.M. Fulrath, J. Am. Ceram. Soc. **54**, 265 (1971)
22. H. Tang, Y.J. Feng, Z. Xu, C.H. Zhang, J.Q. Gao, J. Mater. Res. **24**(5), 1642 (2009)
23. J. Ma, X. Liu, M. Jiang, H. Yang, G. Chen, X. Liu, L. Qin, C. Luo, J. Mater. Sci. Mater. Electron. **25**, 992 (2014)
24. H.T. Martirenat, J.C. Burfoot, J. Phys. C Solid State Phys. **7**, 3182 (1974)
25. A.J. Moulson, J.M. Herbert, *Electroceramics Materials, Properties, Applications*, 2nd edn. (Wiley, New York, 2003)
26. W.Y. Choi, J.-H. Ahn, W.-J. Lee, H.-G. Kim, Mater. Lett. **37**, 119 (1998)
27. W. Li, J. Qi, Y. Wang, L. Li, Z. Gui, Mater. Lett. **57**, 1 (2002)
28. D. Shan, Y. Qu, J. Song, J. Mater. Res. **22**(3), 730 (2007)
29. K. Uchino, S. Nomura, Ferroelectr. Lett. **44**, 55 (1982)
30. Q. Tan, D. Viehland, Ferroelectrics **193**, 157 (1997)
31. H. Yu, H.X. Liu, H. Hao, L.L. Guo, C.J. Jin, Z.Y. Yu, M.H. Cao, Appl. Phys. Lett. **91**, 222911 (2007)
32. K. Shantha, K.B.R. Varma, J. Mater. Res. **14**(2), 476 (1999)
33. J.H. Park, B.K. Kim, K.H. Song, S.J. Park, J. Mater. Sci. Mater. Electron. **6**, 97 (1995)
34. K. Kumar, B. Kumar, Ceram. Int. **38**, 1157 (2012)
35. C.A. Randall, N. Kim, J.P. Kucera, W.W. Cao, T.R. Shrout, J. Am. Ceram. Soc. **81**, 677 (1998)
36. S. Zhang, R. Xia, T.R. Shrout, G. Zang, J. Wang, J. Appl. Phys. **100**, 104108 (2006)
37. M. Demartin, D. Damjanovic, Appl. Phys. Lett. **68**, 3046 (1996)
38. H.X. Fu, R.E. Cohen, Nat. Mater. **403**, 281 (2000)
39. D. Damjanovic, J. Am. Ceram. Soc. **88**, 2663 (2005)
40. IEEE Standard on Piezoelectricity, IEEE Standard 176-1978 (Institute of Electrical and Electronic Engineers, New York, 1978)
41. J. Hao, W. Bai, W. Li, J. Zhai, J. Am. Ceram. Soc. **95**, 1998 (2012)
42. W. Cai, C. Fu, J. Gao, X. Deng, J. Mater. Sci. Mater. Electron. **21**, 317 (2010)
43. S.J. Yoon, S.J. Yoo, J.H. Moon, H.J. Jung, H.J. Kim, J. Mater. Res. **11**, 348 (1996)
44. K. Uchino, *Piezoelectric Ceramics Material, Application, Processing and Properties Handbook of Advanced Ceramics* (Elsevier, Amsterdam, 2003)